Int J Clin Exp Med 2020;13(4):2180-2193
www.ijcem.com /ISSN:1940-5901/IJCEM0106029

Original Article

miRNA-137-3p targets kruppel-like factor 4 gene to inhibit Rap1/p38MAPK signaling in osteoporotic rats

Ke Lu[1], Hongzhen Wang[1], Xiaoyang Wu[2], Chong Li[3], Zhiyong Deng[4]

Departments of [1]Joint Surgery, [2]Gastrointestinal Surgery, [3]Orthopedics, [4]Pathology, Affiliated Kunshan Hospital of Jiangsu University, Suzhou, Jiangsu Province, China

Received December 7, 2019; Accepted December 29, 2019; Epub April 15, 2020; Published April 30, 2020

Abstract: Objective: To investigate the role of miRNA-137-3p and Kruppel-like factor 4 (KLF4) in the regulation of osteoblast proliferation and apoptosis in osteoporotic (OP) rats by zoledronic acid (ZA) via the Rap1/p38MAPK signaling pathway. Methods: Sixty rats were randomly and equally divided into control, Sham, OP and OP + ZA treatment groups. The targeting relationship between miRNA-137-3p and KLF4 was validated by Targetscan and double luciferase reporters. qRT-PCR and western blot were used to detect the expression of miR-137-3p, KLF4, and Rap1/p38MAPK pathway related factors and markers of osteogenic differentiation in femoral tissue and cell lines of each group. MTT assays and flow cytometry were used to detect cell proliferation and apoptosis, respectively. Results: Compared to the control and Sham groups, the OP model group showed significantly lower levels of blood phosphorus and BMD; both in femoral tissue and cell lines, the OP model group showed significantly increased miRNA-137-3p expression, decreased KLF4 expression, inhibited Rap1/p38MAPK pathway activation and the down-regulated expression of osteogenic differentiation markers; leading to the decreased osteoblast proliferation and increased apoptosis rates (all $P<0.05$). All these indices improved following ZA treatment (all $P<0.05$). Compared to blank and negative control groups, miRNA-137-3p expression in the miR-137-3p mimic group was up-regulated, whilst KLF4, p38 MAPK, Rap1 and p-p38 MAPK were down-regulated. si-KLF4 could reverse the effects of miRNA-137-3p inhibition. Conclusion: Inhibiting miRNA-137-3p up-regulates the expression of KLF4, activates Rap1/p38MAPK signaling pathway, and promotes the proliferation of osteoblasts in OP rats treated with ZA, inhibiting osteoblast apoptosis.

Keywords: miRNA-137-3p, KLF4 gene, Rap1/p38MAPK signaling pathway, zoledronic acid, osteoporosis

Introduction

Osteoporosis (OP) is a common type of metabolic bone lesions characterized by reduced bone mass, increased bone fragility and the destruction of the bone microstructures [1]. A decline in osteoblast ability to form new bone, and an increase in osteoclast absorption are the main causes of disease [2]. Zoledronic acid (ZA) is a diphosphate drug that promotes bone formation and inhibits bone resorption. ZA is widely used in the treatment of OP and metastatic bone cancer [3-5].

miRNAs are endogenous, non-coding small RNAs that control the transcription and translation of more than a third of all human genes, regulating a plethora of biological processes including proliferation, apoptosis and differentiation [6]. miRNAs have much utility in disease treatment [7, 8]. Liu et al. found that the expression of miRNA-137 could predict the fracture risk in osteoporotic patients [9]. As key regulators of bone metabolism, osteoblasts are regulated by a range of factors and cytokines [10]. Kruppel-like factor 4 (KLF4) is a member of the KLFs family. Previous studies have found that KLF4 is mainly expressed in the digestive tract, but its expression in bone tissue is significantly increased during osteoblast differentiation [11, 12]. However, the role of miRNAs and their downstream pathway regulation of OP remain poorly characterized.

In this study, we reveal for the first time that miRNA-137-3p targets KLF4 and regulates osteoblast differentiation in osteoporotic rats treated with ZA.

Materials and methods

Animal model construction

Sixty 6-month-old female SD rats of SPF grade, weighing 270±20 g, were selected. Rats were purchased from the Hunan Medical Laboratory Animal Center. Rats were housed at a temperature of 23±4°C, a humidity of 60±5%, and day and night cycles of 12 h. After one week of adaptive feeding, the 60 rats were divided into control (normal control group), Sham operation, OP model and OP + ZA treatment groups (ZA was purchased from Guorui Pharmaceutical Co., Ltd. of SINOPHARM Group), with 15 rats in each group. The OP model was established by bilateral ovariectomy [13]. This study was approved by the Ethical Committee of Kunshan First People's Hospital, Affiliated Kunshan Hospital of Jiangsu University. All rats were fasted for 12 h prior to operation. Based on a dosage of 40 mg/kg, rats were firstly anesthetized with 3% sodium pentobarbital solution (Merck, Shanghai North Connaught Biotechnology Co., Ltd., China). Rats were then fixed on the operating table and a longitudinal incision about 1 cm was made on the dorsal side under sterile conditions. After separating the skin, dorsal muscles were opened from both sides of the spine to expose and remove the ovaries. Residual ovaries were ligated using a surgical line. The muscle layer and skin of rats was sutured and the other ovaries were removed by identical methods following alcohol disinfection. No treatments were performed in the control group. In the Sham group, the ovaries were only exposed instead of excised, and excess adipose tissue was removed and then rats were stitched up. Rats in the Sham, OP and OP + ZA groups were injected with gentamicin sulfate (Cisen Pharmaceutical Co., Ltd., China) intramuscularly for 3 consecutive days to avoid infection. After 7 days of modeling, rats in the OP + ZA treatment group were administered 100 $\mu g \cdot kg^{-1} \cdot d^{-1}$ ZA by gavage [14]. ZA was dissolved in 6 mL of distilled water. Rats in the Sham and OP groups were given identical volumes of normal saline for 40 consecutive days.

After 40 days of intervention, rats were fasted without water for 12 h to prevent rats from reflux and aspiration under anesthesia. Then abdominal aortic blood was taken from each group. The average weight of rats at that time point was 259±18 g. Within 24 hours after abdominal aortic blood was taken, pain, vocalization and even self-mutilation during rest were observed in rats, the above situation is regarded as the end point of humanity. First, the rats were given general anesthesia, and then the rats were executed by cervical dislocation [15]. Cardiac response monitored by electrocardiogram was used to determine death in rats. After that, the femurs of each group were washed with normal saline and fixed with 10% formalin (Shanghai Yuanmu Biotechnology Co., Ltd., China) for reserve.

Determination of blood phosphorus, calcium and BMD

Intraperitoneal anesthesia was performed in the rats by injecting 3% sodium pentobarbital solution (Merck, Shanghai Beino Biotechnology Co., Ltd., China) at a dose of 40 mg/kg. After anesthesia, 6 mL abdominal aortic blood was taken from each group and centrifuged at 300 × g for 15 min to obtain the serum. Serum calcium and phosphorus levels were measured using an automatic biochemical detector (SMT100, Beijing Perlong Medical, China). The BMD of the left femurs was scanned using an American Small Animal Bone Densitometer (Prodigy, American General Electric Medical System, USA) [16]. Exposure parameters: standard mode, current 0.15 mA, voltage 76 kV, time 4:8 (min:sec). BMD was measured using standard software.

Isolation, culture and identification of osteoblasts

The left femoral tissue was taken and superfluous blood vessels and connective tissue were removed. PBS (1 mL) (Beijing Yocon biotechnology Co., Ltd., China) was added. The tissues were cut into 1 mm^3 sections and wash twice under PBS. Tissues were treated with 5 mL 0.25% trypsin (ThermoFisher, USA) and 5 ml 0.1% type II collagenase (GIBCO, USA), and bathed at 37°C for 1 h. After adding M199 medium (3 mL) (Sigma, USA) containing 10% fetal bovine serum, the mixture was centrifuged at 200 × g for 5 min, and the supernatants were discarded. The remaining cells were incubated at 37°C in 5% CO_2 with a further 3 mL of M199 medium containing 10% fetal bovine serum added. Culture medium was refreshed every 2 days and cells in the logarithmic growth phase of the third generation were taken for

subsequent experiments. The morphology of the osteoblasts was imaged on an inverted microscope (IX53, Olympus, Japan).

Alkaline phosphatase (ALP) staining: Cells were treated with ALP color reagent kit (MA0197, Dalian Melone Biotechnology Co., Ltd., China). NBT (20 μL of 150 × stock solution) was added to 3 mL ALP color reaction buffer. After mixing, 30 μL of 100 × BCIP was added to the mixture to form the working solution. Endogenous ALP was detected within 1 h of preparation. Culture medium was removed, cells were washed 3 times with PBS, and fixed in 4% paraformaldehyde (Shanghai Aladdin Biochemical Technology Co., Ltd., China) for 1-2 min. Cells were then washed 3 times in TBST (Beijing Solarbio Science & Technology Co., Ltd., China). After color rendering solution was added, cells were incubated at room temperature for 20 min until the color had developed. Cells were rinsed in PBS and imaged via confocal microscopy.

Alizarin red staining: Cells were further cultured for two weeks to form calcified nodules. Then they were washed twice in PBS, and fixed with 85% ethanol (E-7148, Sigma, Japan) for 10 min. After PBS washing, cells were stained with 0.1% alizarin red solution (Beijing Solarbio Science & Technology Co., Ltd., China) for 10 min and washed with PBS again. Cells were imaged on an inverted microscope.

Zoledronic acid treatment

Third generation osteoblasts isolated from each group were seeded into 96-well plates at a density of $6*10^4$ cells/well in DMEM medium containing 10% fetal bovine serum (Beijing Solarbio Science & Technology Co., Ltd., China). Osteoblasts of the OP + ZA group were treated with 2 μM ZA each day for 3 consecutive days. qRT-PCR, western blot analysis, MTT assays, and flow cytometry were performed.

Cells in the OP + ZA group were transfected and divided into six groups: Blank (no transfection), NC (negative control plasmid), miRNA-137-3p mimic group (miRNA-137-3p mimic), miRNA-137-3p inhibitor group (miRNA-137-3p interfering plasmid), siRNA-KLF4 group (KLF4 interfering plasmid), and miRNA-137-3p inhibitor + si-KLF4 group (miRNA-137-3p interfering plasmid and KLF4 interfering plasmid). All plasmids and inhibitors were purchased from Shanghai Genechem Co., Ltd., China. After digestion with 0.25% trypsin (ThermoFisher, USA), cells were suspended in 10% fetal bovine serum (Gibco, USA) to $1*10^5$/mL and seeded into 96-well plates. When cells reached 70% confluency, the culture medium was replaced with serum-free M199 for continuous culture. The cells were transfected after continuous culture for 24 h. Then 200 μL serum-free OptiMEM medium (Gibco, USA) was mixed respectively with 6 μL of lipofectamine 2000 (Invitrogen, USA) and with 2 μg target plasmids. After 10 min, the two mixtures were mixed and incubated at room temperature for 30 min. The original culture medium was replaced by 1.5 mL serum-free M199 culture medium in each well, and transfection complex was added to each well. The cells were cultured in 37°C and 5% CO_2 incubators for 24 h and then the culture medium was replaced. The cells were collected after 48 h of culture.

Dual luciferase reporter gene experiment

Targetscan was used to predict the target genes of miRNA-137-3p. Dual luciferase reporter assays were used to verify the relationship between KLF4 and miRNA-137-3p. SpeI and Hind III sites were introduced into the pMIR-reporter. Mutant sites of the complementary sequences were designed onto the KLF4 sequence. Following restriction endonuclease digestion, target gene fragments were inserted into the pMIR-reporter plasmid (Kelei biological Technology Co., Ltd., China) using T4 DNA ligase (TAKARA, China). WT and MUT luciferase reporter plasmids (Shanghai Yubo Biology Technology Co., Ltd., China) were co-transfected with miRNA-137-3p in HEK-293T cells (Shanghai Eykits Biotechnology Co., Ltd., China). After 48 h of continuous transfection, the culture medium was left out and the cells were washed with PBS. Cells were collected and lysed. Luciferase activity was tested by dual luciferase reporting system. Firefly luciferase (50 μL) and Ranilla luciferase (50 μL) solutions (Shanghai qcbio Science & Technologies Co., Ltd., China) were added to 10 μL of cell lysate. Relative luciferase activity = firefly luciferase activity/Ranilla luciferase activity.

qRT-PCR

Left femurs were extracted and ground into pulp. Total RNA in the femoral tissue was

Table 1. qRT-PCR primer sequence

Gene	Sequence
miR-137-3p	
Upstream primer	5'-GTGTCTATCTCCCATTGAGG-3'
Downstream primer	5'-CGATGTGAATTCCACAATTGC-3'
KLF4	
Upstream primer	5'-CAGCAAGGTATGGTGTTCAG-3'
Downstream primer	5'-TGCATGCATTTGATATTAGCCT-3'
p38 MAPK	
Upstream primer	5'-GAATCTTAGCCAAGTGAACCAAC-3'
Downstream primer	5'-GGACAGAAGCACCAGAGCTCACA-3'
Rap1	
Upstream primer	5'-CTTCAATCCAAGCCCCTC-3'
Downstream primer	5'-TTCACCGGCCTTCAATTT-3'
ALP	
Upstream primer	5'-GCTGAGGGTCGTCA GACTG-3'
Downstream primer	5'-TCCCATTCTCCGAAATCGCTAT-3'
OPN	
Upstream primer	5'-CGCAGGGAACGTCCTAA-3'
Downstream primer	5'-TCGGGTATCAGTGTGCCGAA-3'
OCN	
Upstream primer	5'-TACGTTCGGACGCAGCTAA-3'
Downstream primer	5'-TCGTGGGCACCTGAAGTATG-3'
U6	
Upstream primer	5'-GTCGCCTTCGGGCACCAA-3'
Downstream primer	5'-GAGAGGGCAGTACCATTCGA-3'
β-actin	
Upstream primer	5'-GGACTCAACTCTACCCTAAT-3'
Downstream primer	5'-AAATCTATCTCGGCATGAGG-3'

Note: KLF4: Kruppel-like factor 4; ALP: alkaline phosphatase; OPN: osteopontin; OCN: osteocalcin.

extracted using the one-step method according to the instructions of Trizol reagent kit (Invitrogen, USA). Ultraviolet absorbances were measured on a spectrophotometer (Shanghai Lab-Spectrum Instruments Co., Ltd., China) at 260 and 280 nm. If the $OD_{260\ nm}/OD_{280\ nm}$ ratio was between 1.8 and 2.0, the purity of the RNA was high. Reverse transcription was performed using commercial reverse transcription kits (Promega, USA). Reaction conditions: 3 min at 70°C, 2 min in the ice bath, 50 min at 37°C, and 10 min at 95°C. cDNA obtained from reverse transcription was stored at -20°C. Primers targeting miR-137-3p, KLF4, p38MAPK, Rap1, ALP, osteopontin (OPN), osteocalcin (OCN), U6 and β-actin (**Table 1**) were designed and synthesized by Shanghai Genechem Co., Ltd. The SYBR Premix EX Taq fluorescence quantitative PCR kit (DRR041A, Takara, China) was used to detect the expression of miR-137-3p and the mRNA of each gene. The reaction system included: RNase Free H_2O (11.7 μL), 2 × Taq MasterMix (5.3 μL), forward and reverse primers (5 μM) 1 μL each, and cDNA (1 μL). Reaction conditions: 95°C pre-denaturation for 5 min; denaturation at 94°C for 30 s; 56°C annealing for 40 s, 72°C extension for 60 s, for a total of 40 cycles. miR-137-3p and mRNA expression of each gene were detected using an ABI 7500 fluorescence quantitative PCR instrument (ABI 7500, ABI, USA). miRNA-137-3p was normalized to U6; KLF4, P38MAPK, Rap1, ALP, OPN and OCN were normalized to β-actin. The relative expression of each target gene was calculated using the $2^{-\Delta\Delta Ct}$ method. The same qRT-PCR method was applied in cell experiments.

Western blot analysis

Left femoral tissue (50 μg) was sectioned, fully lysed in protein lysate solution (Beijing Solarbio Science & Technology Co., Ltd., China) and homogenized at 200 × g. Lysates were cooled for 20 min in an ice bath and centrifuged at 300 × g at 4°C for 30 min. Protein concentrations were determined via BCA protein concentration assay kit (ThermoFisher, USA) and diluted to 1 μg/μL by deionized water. Then 20 μg protein was sampled in each well. Proteins were separated by 10% SDS-PAGE gel (Beijing Solarbio Science & Technology Co., Ltd., China) at 15 v/cm. Proteins were transferred to PVDF membranes by wet transfer. Proteins were labeled with ponceau stain (Shanghai Beyotime Biotechnology Co., Ltd., China). The PVDF membranes were washed with TBST three times, blocked at room temperature with 5% skim milk for 1 h, and washed with TBST again, three times. Membranes were probed with rabbit anti-KLF4 (1-2 μg/mL, ab106629, Abcam, UK), rabbit anti-p38 MAPK (1:1,000, ab31828, Abcam, UK), p-p38MAPK (1:10,000, ab47363, Abcam, UK), rabbit anti-Rap1 (1 μg/mL, ab113480, Abcam, Abcam, UK), rabbit anti-ALP (1 μg/mL, 839, Abcam, UK), rabbit anti-OPN (0.2 μg/mL, ab11503, Abcam, UK), rabbit anti-OCN (5 μg/mL, ab13418, Abcam, UK), and rabbit anti-β-actin

(1:1,000, ab8226, Abcam, UK) primary antibodies were incubated overnight at 4°C. Membranes were washed with TBST three times, for 5 min each time. Membranes were then labeled with HRP-labeled sheep anti-rabbit IgG secondary antibodies (1:2,000, ab6721, Abcam, UK) for 1 h. Membranes were washed with TBST three times, for 5 min each time. DAB was used for color rendering. Proteins were visualized via chemiluminescence (Beckman Coulter, USA). The average absorbance of the sample divided by the average absorbance of the corresponding internal reference was the relative content of the sample protein and the phosphorylated protein. The same western blot method was applied in detecting protein in cells.

MTT assays

Cells in logarithmic growth phase were seeded in 96-well plates at a density of $1*10^5$/well, with 6 parallel wells in each group. Blank control wells with only medium were used as controls. When cells grew to 80% confluency, 10 μL of 5 mg/mL MTT solution (Sigma, USA) was added at 37°C for 3 h. Supernatants were removed and the plate was cleaned once with PBS. Then 150 μL of DMSO (Sigma, USA) was added to each well. After shaking for 10 min, optical density (OD) at 490 nm was measured by enzyme-labeled instrument (Thermo Fisher, USA). Cell viability = (OD of experimental wells - OD of blank wells)/OD of blank wells.

Flow cytometry

Following transfection, cells were digested in trypsinase without EDTA (Beijing Solarbio Science & Technology Co., Ltd., China). Cells were centrifuged at 4°C and 150 × g for 3 min and washed in PBS. Cells were pelleted by centrifugation for 3 min at 150 × g, to discard supernatants, and cell apoptosis was detected using Annexin-V-FITC/PI apoptosis detection kits (Shanghai Beyotime Biotechnology Co., Ltd., China). The cells were washed with binding buffer. Annexin V-FITC + binding buffer and PI + binding buffer were prepared at a ratio of 1:40, respectively. After shaking and mixing, the two mixtures were incubated at room temperature for 30 min, and then they were mixed and continued to incubate for 15 min. Annexin V-FITC and PI fluorescence were detected by flow cytometry (Cytomics™ FC 500, Beckman, Germany) at 488 and 530 nm excitation wavelengths, respectively. Cells in the upper left quadrant represented damaged cells. The lower left quadrant represented normal cells. The upper right quadrant represented late apoptotic and necrotic cells. The lower right quadrant represented cells at the early stages of apoptosis.

Statistical analysis

Data were analyzed using SPSS 21.0 statistical software (SPSS, Inc., Chicago, IL, USA). Measurement data were expressed as the mean ± standard deviation ($\bar{x} \pm$ sd). All experiments were repeated on a minimum of 3 occasions. Data normality was tested using the Kolmogorov-Smirnov method. As for data with a normal distribution, Tukey tests were used for post-hoc test following one way ANOVA in multi-group comparisons. As for data with a skewed distribution, Dunn's post test was used for post-hoc analysis after Kruskal-Wallis tests. $P<0.05$ indicated a significant difference.

Results

Determination of BMD

The BMD of rats in each group were measured at 28 days post-drug intervention. In comparison to the control group, the BMD of rats in the OP model group significantly decreased ($P=0.0015$), as well as the OP + ZA group ($P=0.0168$). Compared to the OP model group, the BMD of the rats treated with ZA increased ($P=0.0058$). There were no significant difference between the BMD in control and Sham groups ($P=0.5526$, **Figure 1**).

Determination of serum phosphorus and serum calcium

After 28 days of drug intervention, serum calcium and phosphorus levels in each group were detected (**Table 2**). Compared to the control group, the levels of serum calcium in the OP and OP + ZA group increased, but the differences were not significant (both $P>0.05$). Serum phosphorus levels were decreased in the OP and OP + ZA groups compared to the control group (both $P<0.05$). Serum phosphorus levels in the OP + ZA group was higher compared to the OP model group ($P<0.05$). There were no significant differences in serum phos-

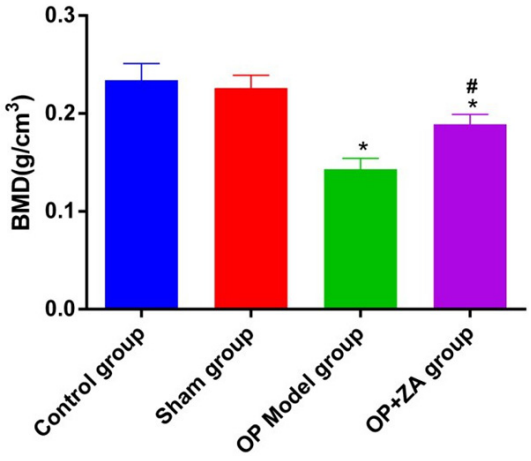

Figure 1. Determination of BMD. BMD: bone mineral density; OP: osteoporosis; ZA: zoledronic acid. Compared with control group, *P<0.05; compared with OP model group, #P<0.05.

Table 2. Determination of serum calcium and serum phosphorus

Group	Blood calcium	Blood phosphorus
Control group	2.73±0.16	2.87±0.23
Sham group	2.67±0.14	2.89±0.26
OP model group	2.73±0.18	2.45±0.22*
OP + ZA group	2.70±0.17	2.65±0.25*,#

Note: OP: osteoporosis; ZA: zoledronic acid; KLF4: Krupel-like factor 4. Compared with control group, *P<0.05; Compared with OP groupmodel group, #P<0.05.

phorus and calcium levels between the control and Sham groups (both P>0.05).

Expression of miRNA-137-3p and mRNA and protein expression of KLF4, genes related to the Rap1/p38MAPK signal pathway in the femoral tissue of rats

Compared to the control group, miR-137-3p expression in the femoral tissues of the OP and OP + ZA group were significantly up-regulated. The mRNA and protein expression levels of KLF4, Rap1 and p38 MAPK were significantly down-regulated, whilst the expression of p-p38 MAPK were also down-regulated (all P<0.05). There were no significant differences between control and Sham groups (all P>0.05). Compared with the OP group, the expression of miR-137-3p in the OP + ZA group was reduced, whilst the mRNA and protein expression of KLF4, Rap1 and p38 MAPK were significantly up-regulated. The levels of active p-p38 MAPK also increased (all P<0.05). These results showed that miR-137-3p expression, KLF4 expression, and Rap1/p38MAPK signaling were inhibited in the OP group, which were improved following ZA treatment (**Figure 2**).

Observation and identification of osteoblasts

After cell culture, the majority of osteoblasts were spindle-shaped or triangular with round or oval nuclei, and the cells were connected with each other and clearly overlapped (**Figure 3A**). ALP staining showed that most nuclei were stained blue, the cytoplasm was mostly gray-white, and black particles were visible in the cytoplasm (**Figure 3B**). Following alizarin red staining, there were clear orange nodules of calcification (**Figure 3C**). This indicated successful osteoblast isolation and culture.

Validation of the relationship between miR-137-3p and KLF4

Through the Targetscan online prediction website, binding sites between miR-137-3p and KLF4 were observed (**Figure 4A**). Dual Luciferase Reporter assays showed that, compared with the NC group, the luciferase activity of the wild type 3'UTR of KLF4 was significantly inhibited by the miRNA-137-3p mimic (P<0.05), whilst luciferase activity of the 3'UTR of KLF4 mutants were not significantly affected by miRNA-137-3p (P>0.05). These results suggested that miR-137-3p specifically bound to wild-type KLF4-3'-UTR, and that KLF4 was the target gene of miR-137-3p.

Expression of miRNA-137-3p and mRNA and protein expression levels of KLF4, Rap1 and p38 MAPK in cells of each group

As shown in **Figure 5**, compared with the control group, the expression of miR-137-3p in the OP model group increased, the expression of KLF4 decreased, and Rap1/p38MAPK signaling was inhibited (all P<0.05). Following ZA treatment, the above indicators improved (all P<0.05). No significant differences between Sham and control groups were observed (all P>0.05).

Following ZA treatment and transfection, no significant differences in the expression of each factor between blank and NC groups were observed (all P>0.05). Compared with blank

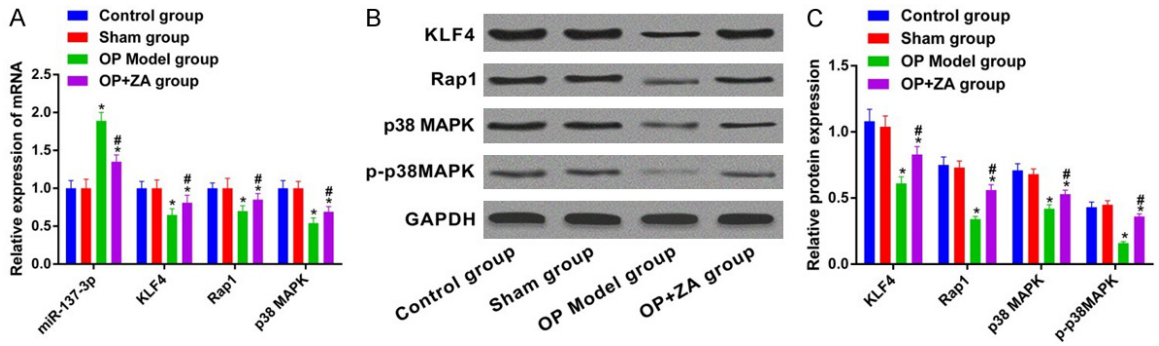

Figure 2. miRNA-137-3p, mRNA and protein expression of KLF4, genes related with Rap1/p38MAPK pathway in femoral tissue. A: Relative expression of mRNA; B: Western blot of protein expression; C: Relative expression of protein; OP: osteoporosis; ZA: zoledronic acid; KLF4: Kruppel-like factor 4. Compared with control group, *P<0.05; Compared with OP model group, #P<0.05.

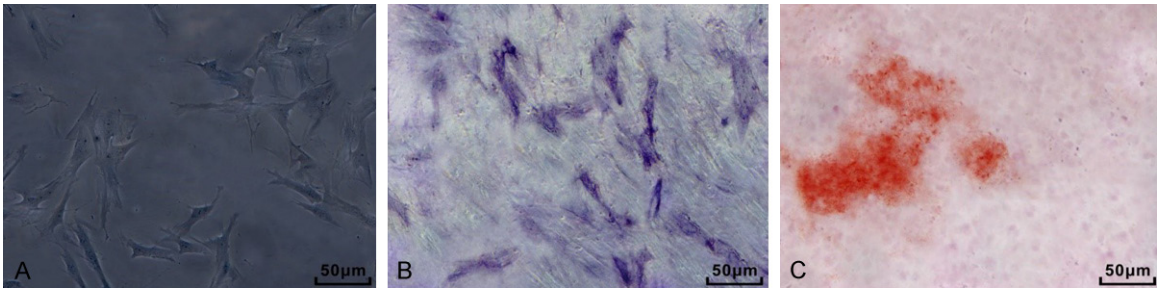

Figure 3. Observation and identification of osteoblasts. A: Morphology of osteoblasts (200 ×); B: Alkaline phosphatase staining of osteoblasts (200 ×); C: Alizarin red staining of osteoblasts (200 ×).

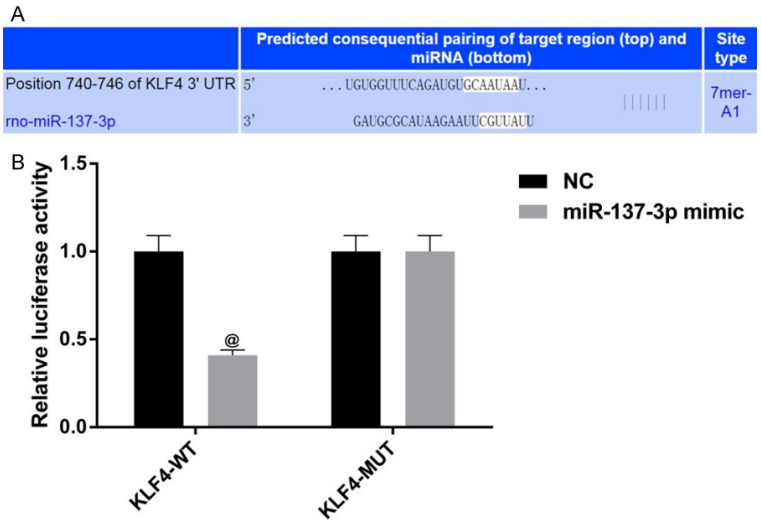

Figure 4. Validation of the relationship between miR-137-3p and KLF4. A: Predictive binding sites of miR-137-3p on 3'UTR of KLF4; B: Double luciferase activity detection; KLF4: Kruppel-like factor 4; NC: negative control; WT: wild type; MUT: mutants. Compared with NC group, @P<0.05.

group, miRNA-137-3p expression in the miR-137-3p mimic group increased, whilst the mRNA and protein expression of KLF4, p38 MAPK and Rap1 in miR-137-3p mimic and si-KLF4 groups decreased. The expression of p-p38 MAPK in both groups also decreased (all P<0.05). In the miR-137-3p inhibitor group, miR-137-3p expression was down-regulated, whilst the mRNA and protein expression of KLF4, p38 MAPK and Rap1 increased. p-p38 MAPK expression was also up-regulated (all P<0.05). The expression of miR-137-3p decreased in the miR-137-3p inhibitor + si-KLF4 group (P< 0.05), and no significant differences were observed amongst other factors (all P>0.05). These results confirmed that miRNA-137-3p inhibited the expression of KLF4 and the activation of Rap1/p38MAPK signaling pathway (**Figure 6**).

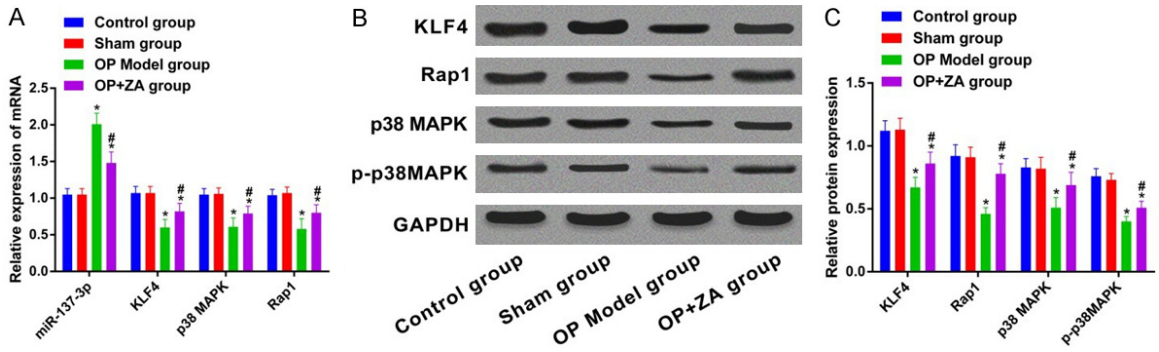

Figure 5. miRNA-137-3p, mRNA and protein expression of KLF4, genes related with Rap1/p38MAPK pathway of each group. A: Relative expression of mRNA; B: Western blot of protein expression; C: Relative expression of protein; OP: osteoporosis; ZA: zoledronic acid; KLF4: Kruppel-like factor 4. Compared with control group, *P<0.05; Compared with OP model group, #P<0.05.

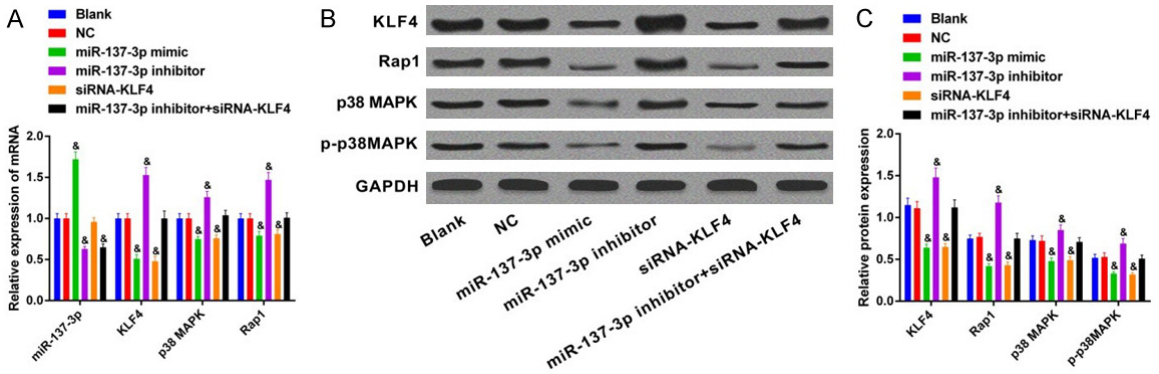

Figure 6. miRNA-137-3p, mRNA and protein expression of KLF4, genes related with Rap1/p38MAPK pathway of OP + ZA group. A: Relative expression of mRNA; B: Western blot of protein expression; C: Relative expression of protein; OP, osteoporosis; ZA, zoledronic acid; KLF4, Kruppel-like factor 4; NC, negative control. Compared with blank group, &P<0.05.

mRNA and protein expression of osteoblast differentiation markers in each group

As shown in **Figure 7**, compared with the control group, the expression of bone differentiation markers in the OP model group significantly decreased (all P<0.05), and improved after ZA treatment (all P<0.05). There were no significant differences in the content of bone differentiation markers between the Sham and control groups (all P>0.05).

After transfection of osteoblasts treated with ZA, no significant differences in the expression of each factor between the blank and NC group were observed (all P>0.05). Compared to the blank group, the mRNA and protein expression of ALP, OPN and OCN in the miR-137-3p mimic group were down-regulated (all P<0.05), whilst these factors were upregulated in the miR-137-3p inhibitor group (all P<0.05). This suggested that miR-137-3p inhibited KLF4 expression and osteoblast differentiation (**Figure 8**).

Changes in cell proliferation ability post-transfection

As shown in **Figure 9**, compared to the control group, the cell viability of the OP model group decreased significantly at 48 h and 72 h (both P<0.05), and improved significantly after ZA treatment (both P<0.05). There were no significant differences between Sham and control groups at any time point (both P>0.05).

Transfection of OP + ZA treatment groups showed no significant differences in OD values at any time point between NC and blank groups (both P>0.05). Compared to blank group, cell proliferation decreased in the miR-137-3p mimic and si-KLF4 groups (both P<0.05); cell proliferation significantly increased in the miR-

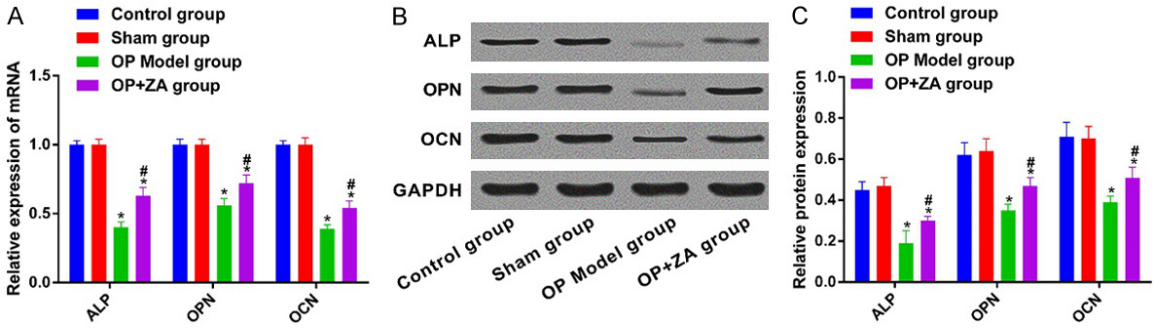

Figure 7. Expression of mRNA and protein of ALP, OPN, OCN in cells of each group. A: Relative expression of mRNA; B: Western blot of protein expression; C: Relative expression of protein; OP: osteoporosis; ZA: zoledronic acid; ALP: alkaline phosphatase; OPN: osteopontin; OCN: osteocalcin. Compared with control group, *P<0.05; Compared with OP model group, #P<0.05.

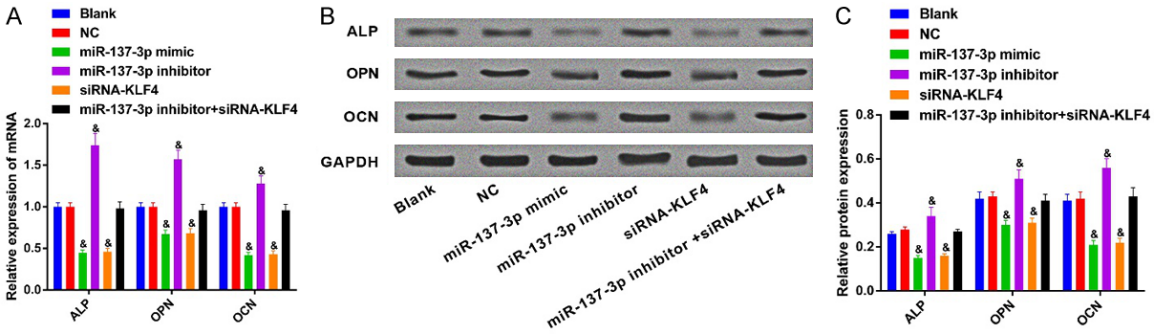

Figure 8. mRNA and protein of ALP, OPN, OCN in cells of OP + ZA group. A: Relative expression of mRNA; B: Western blot of protein expression; C: Relative expression of protein; OP: osteoporosis; ZA: zoledronic acid; NC: negative control; ALP: alkaline phosphatase; OPN: osteopontin; OCN: osteocalcin. Compared with blank group, &P<0.05.

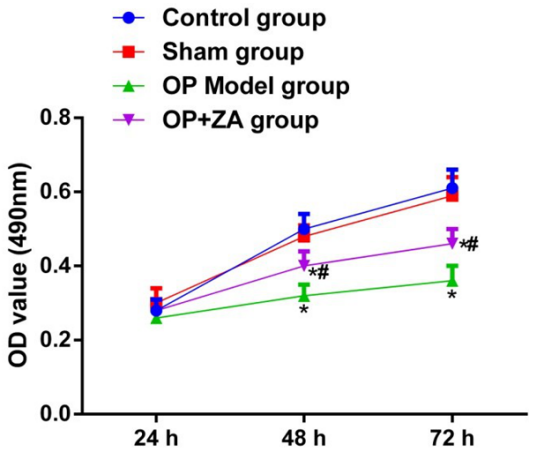

Figure 9. Comparison of proliferation ability in cells of each group. OP: osteoporosis; ZA: zoledronic acid; OD: optical density. Compared with control group, *P<0.05; Compared with OP model group, #P<0.05.

137-3p inhibitor group, but had no significant change in the miR-137-3p inhibitor + si-KLF4 group (all P>0.05). These results confirmed that miR-137-3p inhibited the proliferation of OP in osteoblasts treated with ZA, and that KLF4 promotes osteoblast proliferation (**Figure 10**).

Cell apoptosis detected by flow cytometry

As shown in **Figure 11**, compared with the control group, the apoptosis rates of cells in the OP significantly increased (P<0.05), and improved after ZA treatment (P<0.05). There were no significant differences in apoptosis rates between Sham and control groups (P>0.05).

Further transfection showed no significant differences in apoptosis rates between the NC and blank groups (P>0.05). Compared with the blank group, apoptosis rates in the miR-137-3p mimic and siRNA-KLF4 group significantly increased (both P<0.05). Apoptosis in the miR-137-3p inhibitor group significantly decreased (both P<0.05), but the miR-137-3p inhibitor + si-KLF4 group showed no significant changes

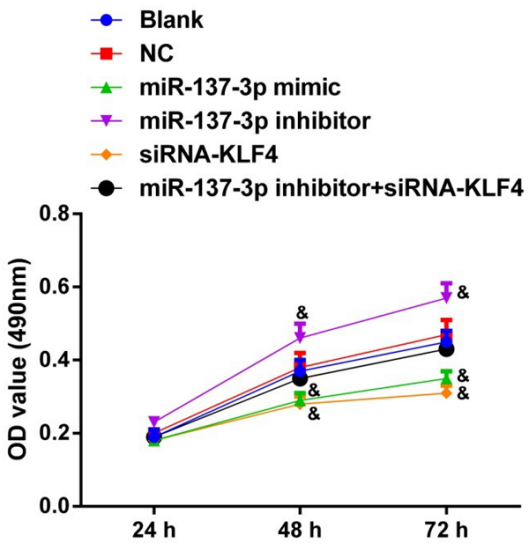

Figure 10. Comparison of proliferation ability in cells of each subgroup of OP + ZA group. OP: osteoporosis; ZA: zoledronic acid; OD: optical density; NC: negative control. Compared with blank group, $^{\&}P<0.05$.

(both P>0.05). These results suggested that miR-137-3p promotes the apoptosis of osteoblasts in OP rats treated with ZA, and that KLF4 inhibits osteoblast apoptosis (**Figure 12**).

Discussion

As a third generation diphosphate drug, ZA has the advantage of long drug intervals and low digestive tract reactions [17]. An intravenous drip of ZA in patients with OP can effectively reduce brittle fractures and improve BMD [18, 19]. Osteoblasts are the major functional cells involved in bone mineralization, bone reconstruction, and bone matrix secretion during bone formation. If the function or number of osteoblasts decreases, the risk of fracture increases and OP occurs [20, 21]. In recent years, studies on the roles of specific miRNAs during bone metabolism have attracted increasing attention, and it is now fully accepted that miRNAs participate in the proliferation and apoptosis of osteoblasts [22, 23]. In this study, an OP rat model was constructed and it was found that miR-137-3p regulates KLF4 and Rap1/p38MAPK pathways, thus participating in the treatment of OP rats by ZA, and regulating the proliferation and apoptosis of OP rat osteoblasts.

BMD refers to the levels of bone per unit area or volume and is the gold standard for the diagnosis of OP [24, 25]. In this study, BMD of the OP model group and OP + ZA treatment group decreased in comparison to control groups, whilst the BMD of rats treated with ZA improved. Phosphorus is a major bone mineral that maintains mechanical strength [26, 27]. We found that the serum phosphorus content of OP model rats significantly decreased, which may be related to the decreased estrogen after ovariectomy. The serum phosphorus content increased following ZA treatment.

miRNAs play important roles in cell growth and development and are emerging as key regulators of bone metabolism, osteoblast growth, differentiation and biological activity [28, 29]. Changes in miRNA expression can cause OP, and drugs that regulate bone metabolism interfere with miRNA expression [22-30]. miRNA-137 is located on chromosome 1p22 and its expression is down-regulated in non-small cell lung cancer, ovarian cancer, and cervical cancer [31-33]. A recent study on OP fractures found that the expression of miR-137 in isolated cells of patients with OP fractures was significantly up-regulated, whilst ALP activity was inhibited [10]. This implicated that the imbalance of expression of miRNA-137 may be related to the pathogenesis of OP. In this study, the expression of miRNA-137-3p, KLF4 and Rap1/p38MAPK pathway-related factors in the femoral tissues of three groups of rats were further determined. MiRNA-137-3p overexpressed in the OP group, but KLF4, and Rap1/p38MAPK expression in the OP group were inhibited, which can be recovered following ZA treatment. ZA is a common regulator of bone metabolism. We confirmed that ZA down-regulates the expression of miR-137-3p to regulate OP. KLF4 is highly expressed in bone tissue and its overexpression reduces the differentiation of osteoclasts and osteoblasts, disrupting bone homeostasis [12]. In this study, we found that osteoblasts and their downstream signaling pathways were highly sensitive to miR-137-3p.

We successfully isolated rat osteoblasts which we confirmed with ALP and alizarin red staining. Compared to control and Sham groups, miR-137-3p expression in OP group was enhanced, whilst KLF4 and Rap1/p38MAPK were inhibited. The proliferation of osteoblasts was significantly inhibited in the OP model group, but ZA treatment could significantly improve these indicators. Cells of rats in the OP + ZA treat-

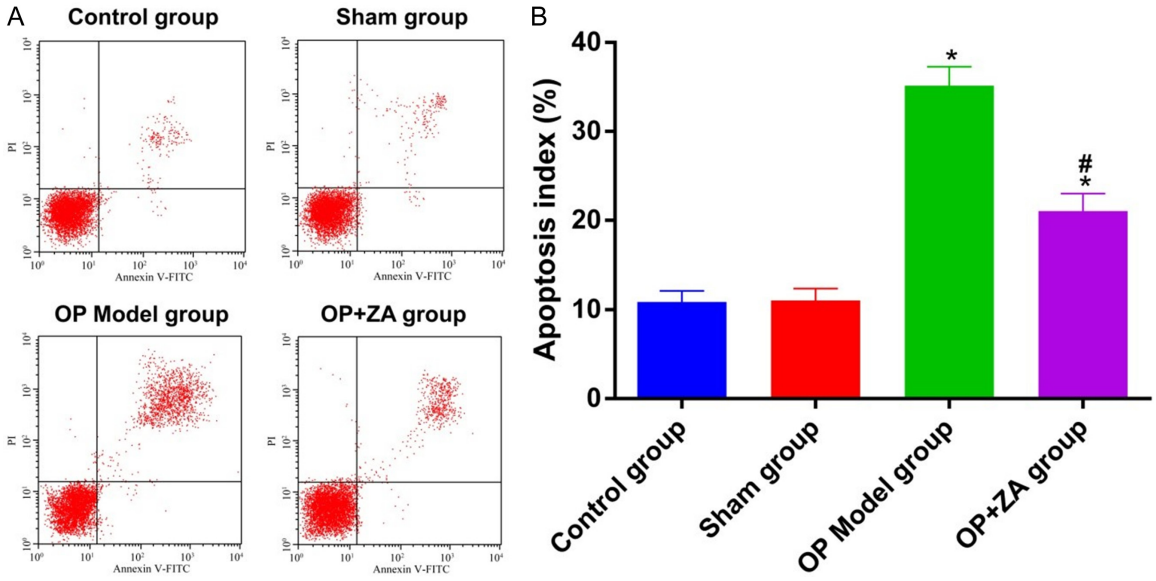

Figure 11. Comparison of cell cycle distribution and apoptotic rate of each group post-transfection. A: Apoptotic detection by flow cytometry; B: Percentage of apoptosis; OP: osteoporosis; ZA: zoledronic acid. Compared with control group, $^{*}P<0.05$; Compared with OP model group, $^{\#}P<0.05$.

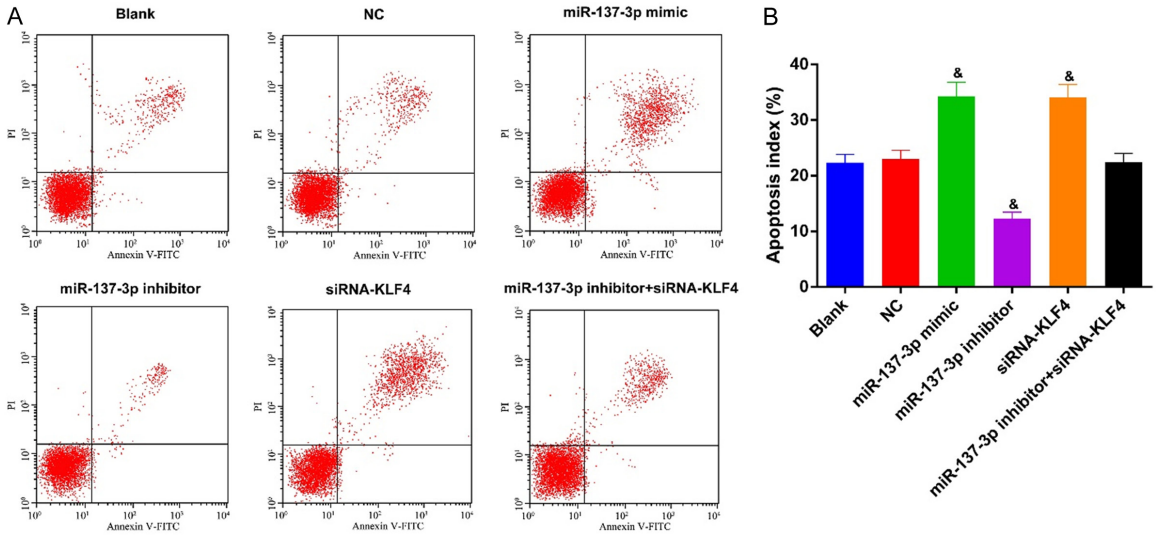

Figure 12. Comparison of cell cycle distribution and apoptotic rate of each subgroup of OP + ZA group post-transfection. A: Apoptotic detection by flow cytometry; B: Percentage of apoptosis; OP: osteoporosis; ZA: zoledronic acid; NC: negative control. Compared with blank group, $^{\&}P<0.05$.

ment group were further transfected and miR-137-3p, KLF4 and Rap1/p38MAPK expression in each group were assessed. The expression of KLF4, p38MAPK and Rap1 in the miR-137 mimic and si-KLF4 groups were down-regulated, whilst the expression of KLF4 and Rap1/p38MAPK pathway-related factors in the miR-137 inhibitor + si-KLF4 group did not change significantly, suggesting that miR-137-3p inhibits the expression of KLF4 and the activation of Rap1/p38MAPK. Studies have confirmed that the activation of p38MAPK signaling up-regulates the level of BMP2 and BMP4, promotes the expression of osteogenic genes, and regulates osteoblast differentiation [34]. In addition, inhibiting the expression of miR-182-5p activates Rap1 signaling and promotes the proliferation and differentiation of OP rat osteo-

blasts, which is of great significance in the treatment of OP [35]. We further confirmed that miR-137-3p can target KLF4 and regulate Rap1/p38MAPK signaling. ALP, OPN and OCN are markers of osteogenic differentiation [36]. The overexpression of miR-137-3p inhibited KLF4 and the expression of markers of osteoblastic differentiation. MTT assays and flow cytometry experiments confirmed that miR-137-3p inhibited the expression of KLF4, inhibiting the proliferation of osteoblasts, and promoting osteoblast apoptosis.

In this study, the regulatory mechanisms of miR-137-3p targeting KLF4 on the proliferation and apoptosis of OP rat osteoblasts were discussed at the cellular level. However, other factors related to OP, including mineralized nodules and osteoclasts, were not discussed in detail. In addition, whether ZA regulates the biological behavior of OP osteoblasts by regulating other small RNAs or pathways other than miR-137-3p requires further discussion.

In conclusion, we have demonstrated that the over-expression of miRNA-137-3p inhibits the expression of KLF4, and regulates the biological characteristics of osteoblasts in OP rats through the construction of an OP rat model. Moreover, this study suggests that this regulation is related to Rap1/p38MAPK signaling, further clarifying the biological mechanism of OP. It is hoped that OP therapeutics can be further improved by ZA combined with targeted therapy.

Acknowledgements

This work was supported by the Beijing Bethune Charitable Foundation (B19337ES).

Disclosure of conflict of interest

None.

Address correspondence to: Zhiyong Deng, Department of Pathology, Affiliated Kunshan Hospital of Jiangsu University, No. 91 Qianjin West Road, Suzhou 215300, Jiangsu Province, China. Tel: +86-05-12-57592630; Fax: +86-0512-57592630; E-mail: dongqirong15l@163.com

References

[1] Nayak S and Greenspan SL. Osteoporosis treatment efficacy for men: a systematic review and meta-analysis. J Am Geriatr Soc 2017; 65: 490-495.

[2] Bilousova G, Jun du H, King KB, De Langhe S, Chick WS, Torchia EC, Chow KS, Klemm DJ, Roop DR and Majka SM. Osteoblasts derived from induced pluripotent stem cells form calcified structures in scaffolds both in vitro and in vivo. Stem Cells 2011; 29: 206-216.

[3] Zhao B, Zhao W, Wang Y, Zhao Z, Zhao C, Wang S and Gao C. Prior administration of vitamin K2 improves the therapeutic effects of zoledronic acid in ovariectomized rats by antagonizing zoledronic acid-induced inhibition of osteoblasts proliferation and mineralization. PLoS One 2018; 13: e0202269.

[4] Wiedemann A, Renard E, Hernandez M, Dousset B, Brezin F, Lambert L, Weryha G and Feillet F. Annual injection of zoledronic acid improves bone status in children with cerebral palsy and rett syndrome. Calcif Tissue Int 2019; 104: 355-363.

[5] Liu J, Pathak JL, Hu X, Jin Y, Wu Z, Al-Baadani MA, Wu S, Zhang H, Farkasdi S, Liu Y, Ma J and Wu G. Sustained release of zoledronic acid from mesoporous TiO(2)-layered implant enhances implant osseointegration in osteoporotic condition. J Biomed Nanotechnol 2018; 14: 1965-1978.

[6] Panwar B, Omenn GS and Guan Y. miRmine: a database of human miRNA expression profiles. Bioinformatics 2017; 33: 1554-1560.

[7] Sambandan S, Akbalik G, Kochen L, Rinne J, Kahlstatt J, Glock C, Tushev G, Alvarez-Castelao B, Heckel A and Schuman EM. Activity-dependent spatially localized miRNA maturation in neuronal dendrites. Science 2017; 355: 634-637.

[8] Telonis AG, Magee R, Loher P, Chervoneva I, Londin E and Rigoutsos I. Knowledge about the presence or absence of miRNA isoforms (isomiRs) can successfully discriminate amongst 32 TCGA cancer types. Nucleic Acids Res 2017; 45: 2973-2985.

[9] Liu X and Xu X. MicroRNA-137 dysregulation predisposes to osteoporotic fracture by impeding ALP activity and expression via suppression of leucine-rich repeat-containing G-protein-coupled receptor 4 expression. Int J Mol Med 2018; 42: 1026-1033.

[10] Dong J, Cui X, Jiang Z and Sun J. MicroRNA-23a modulates tumor necrosis factor-alpha-induced osteoblasts apoptosis by directly targeting Fas. J Cell Biochem 2013; 114: 2738-2745.

[11] Ghaleb AM and Yang VW. Kruppel-like factor 4 (KLF4): what we currently know. Gene 2017; 611: 27-37.

[12] Kim JH, Kim K, Youn BU, Lee J, Kim I, Shin HI, Akiyama H, Choi Y and Kim N. Kruppel-like factor 4 attenuates osteoblast formation, func-

tion, and cross talk with osteoclasts. J Cell Biol 2014; 204: 1063-1074.
[13] Griffith JF, Wang YX, Zhou H, Kwong WH, Wong WT, Sun YL, Huang Y, Yeung DK, Qin L and Ahuja AT. Reduced bone perfusion in osteoporosis: likely causes in an ovariectomy rat model. Radiology 2010; 254: 739-746.
[14] Yishake M, Yasen M, Jiang L, Liu W, Xing R, Chen Q, Lin H and Dong J. Effects of combined teriparatide and zoledronic acid on posterior lumbar vertebral fusion in an aged ovariectomized rat model of osteopenia. J Orthop Res 2018; 36: 937-944.
[15] Herrmann K and Flecknell P. The application of humane endpoints and humane killing methods in animal research proposals: a retrospective review. Altern Lab Anim 2018; 46: 317-333.
[16] Keiler AM, Zierau O, Vollmer G, Scharnweber D and Bernhardt R. Estimation of an early meaningful time point of bone parameter changes in application to an osteoporotic rat model with in vivo microcomputed tomography measurements. Lab Anim 2012; 46: 237-244.
[17] Frank E. Treatment of low bone density or osteoporosis to prevent fractures in men and women. Ann Intern Med 2017; 167: 899.
[18] Tu CW, Huang KF, Hsu HT, Li HY, Yang SS and Chen YC. Zoledronic acid infusion for lumbar interbody fusion in osteoporosis. J Surg Res 2014; 192: 112-116.
[19] Majithia N, Atherton PJ, Lafky JM, Wagner-Johnston N, Olson J, Dakhil SR, Perez EA, Loprinzi CL and Hines SL. Zoledronic acid for treatment of osteopenia and osteoporosis in women with primary breast cancer undergoing adjuvant aromatase inhibitor therapy: a 5-year follow-up. Support Care Cancer 2016; 24: 1219-1226.
[20] An J, Yang H, Zhang Q, Liu C, Zhao J, Zhang L and Chen B. Natural products for treatment of osteoporosis: the effects and mechanisms on promoting osteoblast-mediated bone formation. Life Sci 2016; 147: 46-58.
[21] Solberg LB, Brorson SH, Stordalen GA, Baekkevold ES, Andersson G and Reinholt FP. Increased tartrate-resistant acid phosphatase expression in osteoblasts and osteocytes in experimental osteoporosis in rats. Calcif Tissue Int 2014; 94: 510-521.
[22] Liu XD, Cai F, Liu L, Zhang Y and Yang AL. MicroRNA-210 is involved in the regulation of postmenopausal osteoporosis through promotion of VEGF expression and osteoblast differentiation. Biol Chem 2015; 396: 339-347.
[23] Zhang S, Wu W, Jiao G, Li C and Liu H. MiR-455-3p activates Nrf2/ARE signaling via HDAC2 and protects osteoblasts from oxidative stress. Int J Biol Macromol 2018; 107: 2094-2101.
[24] Kurland ES, Cosman F, McMahon DJ, Rosen CJ, Lindsay R and Bilezikian JP. Parathyroid hormone as a therapy for idiopathic osteoporosis in men: effects on bone mineral density and bone markers. J Clin Endocrinol Metab 2000; 85: 3069-3076.
[25] Zhang ZQ, Ho SC, Chen ZQ, Zhang CX and Chen YM. Reference values of bone mineral density and prevalence of osteoporosis in Chinese adults. Osteoporos Int 2014; 25: 497-507.
[26] Heaney RP, Recker RR, Watson P and Lappe JM. Phosphate and carbonate salts of calcium support robust bone building in osteoporosis. Am J Clin Nutr 2010; 92: 101-105.
[27] Park SE, Oh KW, Lee WY, Baek KH, Yoon KH, Son HY, Lee WC and Kang MI. Association of osteoporosis susceptibility genes with bone mineral density and bone metabolism related markers in Koreans: the Chungju Metabolic Disease Cohort (CMC) study. Endocr J 2014; 61: 1069-1078.
[28] Zhang X, Zhu Y, Zhang C, Liu J, Sun T, Li D, Na Q, Xian CJ, Wang L and Teng Z. miR-542-3p prevents ovariectomy-induced osteoporosis in rats via targeting SFRP1. J Cell Physiol 2018; 233: 6798-6806.
[29] Ahn TK, Kim JO, Kumar H, Choi H, Jo MJ, Sohn S, Ropper AE, Kim NK and Han IB. Polymorphisms of miR-146a, miR-149, miR-196a2, and miR-499 are associated with osteoporotic vertebral compression fractures in Korean postmenopausal women. J Orthop Res 2018; 36: 244-253.
[30] van Wijnen AJ, van de Peppel J, van Leeuwen JP, Lian JB, Stein GS, Westendorf JJ, Oursler MJ, Im HJ, Taipaleenmaki H, Hesse E, Riester S and Kakar S. MicroRNA functions in osteogenesis and dysfunctions in osteoporosis. Curr Osteoporos Rep 2013; 11: 72-82.
[31] Zhang B, Liu T, Wu T, Wang Z, Rao Z and Gao J. microRNA-137 functions as a tumor suppressor in human non-small cell lung cancer by targeting SLC22A18. Int J Biol Macromol 2015; 74: 111-118.
[32] Li X, Chen W, Zeng W, Wan C, Duan S and Jiang S. microRNA-137 promotes apoptosis in ovarian cancer cells via the regulation of XIAP. Br J Cancer 2017; 116: 66-76.
[33] Zhang H, Yan T, Liu Z, Wang J, Lu Y, Li D and Liang W. MicroRNA-137 is negatively associated with clinical outcome and regulates tumor development through EZH2 in cervical cancer. J Cell Biochem 2018; 119: 938-947.
[34] Wang L, Li JY, Zhang XZ, Liu L, Wan ZM, Li RX and Guo Y. Involvement of p38MAPK/NF-kappaB signaling pathways in osteoblasts differ-

entiation in response to mechanical stretch. Ann Biomed Eng 2012; 40: 1884-1894.

[35] Pan BL, Tong ZW, Li SD, Wu L, Liao JL, Yang YX, Li HH, Dai YJ, Li JE and Pan L. Decreased microRNA-182-5p helps alendronate promote osteoblast proliferation and differentiation in osteoporosis via the Rap1/MAPK pathway. Biosci Rep 2018; 38.

[36] Wu L, Qi H, Zhong Y, Lv S, Yu J, Liu J, Wang L, Bi J, Kong X, Di W, Zha J, Liu F and Ding G. 11beta-Hydroxysteroid dehydrogenase type 1 selective inhibitor BVT.2733 protects osteoblasts against endogenous glucocorticoid induced dysfunction. Endocr J 2013; 60: 1047-1058.